The Distribution of Stratospheric Column Ozone (SCO) Determined from Satellite Observations: Validation of Solar Backscattered Ultraviolet (SBUV) Measurements in Support of the Tropospheric Ozone Residual (TOR) Method

Amy E. Wozniak[1,2,3]

Jack Fishman[1]

Pi-Huan Wang[1,4]

John K. Creilson[1,2]

[1] NASA Langley Research Center, Hampton, Virginia
[2] Also at SAIC, Hampton, Virginia
[3] NASA Goddard Space Flight Center, Greenbelt, Maryland
[4] Also at Science and Technology Corporation, Hampton, Virginia

Submitted to
Journal of Geophysical Research (Atmospheres)
August 4, 2004

The global (50°N – 50°S) distribution of stratospheric column ozone (SCO) is derived using SBUV profiles and compared with SCO amounts derived from SAGE and ground-based measurements. An evaluation of archived SBUV (Version 6) ozone profiles with ozonesonde profiles shows that the low resolution of the SBUV instrument in the troposphere and lower stratosphere leads to a low bias in the SBUV profile in the troposphere and a high bias in the lower stratosphere in regions where anthropogenic tropospheric ozone production influences the climatology. An empirical correction applied to the SBUV profile prior to separating the stratosphere from the troposphere reduces the bias in the lower stratosphere and results in a SCO distribution in good agreement with SCO derived from SAGE ozone profiles. Because the empirical correction is most pronounced at northern middle latitudes we compare these resultant SCO values with those measured at two northern middle latitude sites (Wallops Island and Hohenpeissenberg) using concurrent measurements from Dobson spectrophotometers and ozonesondes. Our analysis shows that the empirically corrected SCO at these sites captures the seasonal cycle of SCO as well as the seasonal cycle derived from SAGE stratospheric ozone profiles. These results have important implications for the derivation of tropospheric ozone derived from SBUV ozone profiles in conjunction with TOMS total ozone measurements using the tropospheric ozone residual (TOR) methodology.

1. Introduction

Determination of the global distribution of tropospheric ozone is central to gaining a fundamental understanding of tropospheric chemistry and to assessing how human activity has perturbed the composition of the pre-industrial atmosphere [e.g., see Crutzen, 1974; Fishman and Crutzen, 1978]. Attempts to produce a global distribution were first described in a series of studies in the 1970's using data from surface stations [Fabian and Pruchniewicz, 1973; 1977] and subsequently from analyses of ozonesonde measurements [Chatfield and Harrison, 1977; Fishman et al., 1979]. Because of the variability inherently present in its distribution and abundance, Prinn [1988] recognized the difficulty in obtaining a representative depiction of tropospheric ozone by using only surface and ozonesonde measurements and suggested that a considerable international effort be initiated to derive an accurate global picture using conventional in situ measurement techniques. To date, however, the establishment of an effective monitoring network is still not in place, and many regions on the planet are significantly undersampled. Subsequently, an alternative approach to derive a global picture of tropospheric ozone using satellite information was introduced by Fishman et al., [1990] using concurrent observations of total ozone and a stratospheric ozone profile from independent satellite instruments to derive a quantity called the tropospheric ozone

residual (TOR). Although the TOR did not yield any information about the vertical distribution of ozone within the troposphere, it did provide unique insight into the latitudinal, longitudinal and seasonal variability of the column abundance of tropospheric ozone.

Global data sets of atmospheric trace gases using satellite observations have been primarily constrained to distributions in the stratosphere [Kaye and Fishman, 2003] since making measurements at these relatively higher altitudes is much simpler than in the troposphere. Validation of these stratospheric data products has been critical to the assessment of stratospheric ozone depletion and a monumental amount of research has been conducted to assess the accuracy of stratospheric ozone derived from satellites as well as determining how well various satellite techniques compare to one another [World Meteorological Organization (WMO), 1999; WMO, 2003]. Thus, we describe how relatively abundant stratospheric ozone profiles from satellite instruments such as SAGE (Stratospheric Aerosol and Gas Experiment) and SBUV (Solar Backscattered Ultraviolet) have been used to derive global TOR distributions, and then, as an alternative to explicitly validating the global TOR distribution, we assess the other component that comes out of TOR derivation, namely the global distribution of stratospheric column ozone (SCO). In the following sections we describe the methodology for deriving SCO from SBUV measurements, and validate the SBUV SCO through a comparison with SCO derived from SAGE measurements and with a comparable SCO quantity derived from concurrent ozonesonde and ground-based total ozone measurements.

2. The TOR Method

The first TOR described in Fishman et al. [1990] used concurrent observations of total ozone from TOMS (Total Ozone Mapping Spectrometer) and stratospheric ozone profiles from SAGE to generate climatological maps of tropospheric column ozone. These depictions provided insight into how the seasonal tropospheric ozone distribution was influenced on hemispheric spatial scales by biomass burning in southern Africa and South America in the Southern Hemisphere, and by anthropogenic pollution sources from North America and Europe [Fishman et al., 1990]. Whereas using TOMS and stratospheric ozone profile data from SAGE and SAGE II archives could generate

climatological TOR maps, generation of TOR fields with better temporal resolution requires a higher sampling frequency than the 30 daily occultations available from the SAGE instruments [Vukovich et al., 1996]. The 40-day period required by SAGE to acquire pole-to-pole coverage, precludes the possibility for deriving synoptic pictures on shorter time scales.

The eruption of Mount Pinatubo in June 1991 prohibited the SAGE instrument from making accurate measurements in the lower stratosphere, and thus TOR fields from concurrent measurements from TOMS and SBUV were derived for comparison with field measurements from NASA's 1992 Transport and Atmospheric Chemistry near the Equator - Atlantic (TRACE-A) mission [Fishman et al., 1996b], a field campaign motivated by the first TOMS/SAGE TOR findings of elevated ozone over the tropical South Atlantic Ocean [Fishman et al., 1996a]. The advantage of using SBUV data to derive stratospheric information for generating daily TOR fields is the global horizontal coverage (700-800 profiles daily) provided by the instrument. On the other hand, this method has also been shown to have significant shortcomings if archived (version 6) SBUV data are used [Vukovich et al., 1996; Ziemke at al., 1998].

Because of these noted shortcomings in the archived SBUV data, Fishman and Balok [1999] modified the archived SBUV profiles in the lower atmosphere by applying an "empirical correction" to the lowest three layers of the profiles. The Fishman and Balok study focused on the regional distribution of tropospheric ozone over the eastern United States and used ozonesonde information from Wallops Island (Virginia) to apply "corrections" to every archived SBUV profile used in the study. The empirical correction technique was then expanded to a global domain (from 50°N to 50°S) in Fishman et al. [2003] where the analyses derived by Logan [1999] were used to modify the archived SBUV profiles. The TOR derived from TOMS and empirically corrected SBUV profiles (EC-TOR) made it possible to identify tropospheric regional scale ozone enhancements over northern India and China [Fishman et al., 2003].

3. Validation of the TOR Method and Purpose of this Study

Since Fishman et al. [1990], there have been a number of studies that have used variations of the original TOMS/SAGE approach [Ziemke et al., 1998; Hudson and

Thompson, 1998; Newchurch et al., 2001, 2003]. Each technique uses TOMS measurements to derive total column ozone and an additional measurement to define the stratospheric component of the total column to determine tropospheric ozone. The recent commentary by deLaat and Aben [2003] and subsequent discussion [Fishman, 2003] highlights the difficulty of validating TOR data against currently available databases. Validation of its distribution is extremely difficult and requires the deployment of instruments capable of measuring ozone columns throughout the entire troposphere (i.e., ozonesondes, aircraft profiles and UV-DIAL lidar measurements; see Fishman et al., 1996a,b). Sun [2002] presented an excellent discussion on the accuracy of the TOR method when compared to ozonesonde measurements and he has provided an analysis to show how each method varies with one another. He concludes that each of the six methods display comparable differences when compared with data from tropical ozonesonde stations (the region of interest in his study). Although each of the techniques was able to discern higher values over the Atlantic than over the Pacific, Sun noted that all the methods tend to underestimate the amount of ozone over the Atlantic. The study goes on to conclude that all TOMS-based methods seem to capture the variance better than the absolute amount including seasonal variance. The accuracy of the empirical correction technique of Fishman et al. [2003], the focus of this study, was not included as part of the comparison in Sun [2002].

Subsequently, deLaat and Aben [2003] questioned the accuracy of the EC-TOR fields presented in Fishman et al. [2003] and the finding of the regional nature of enhanced tropospheric ozone amounts at subtropical and northern middle-latitude locations. As pointed out by Fishman [2003], validation of TOR fields is extremely difficult without intensive dedicated field missions. On the other hand, the other product produced in the generation of the EC-TOR, namely the SCO, can be compared against available measurements derived from both *in situ* and satellite techniques. In turn, these satellite measurements have undergone intensive scrutiny since they have been used to assess how much ozone has been destroyed due to the release of chlorofluorocarbons [WMO, 1999; WMO, 2003]. Since EC-TOR uniquely provides a long-term data set at middle latitudes in addition to low latitudes (the limitations of other TOR techniques) a more robust comparison can be preformed because of the much larger set of

measurements (i.e., including NH mid-latitude ozonesonde/ground-based sites) against which the EC-TOR can be compared. In Fishman and Balok [1999], it has already been shown how the EC-TOR agreed much better with ozonesonde data than the TOR using archived SBUV data. In the following sections, we will additionally show how the empirical correction to the SBUV archive has improved the accuracy of the SCO derived from the EC-TOR methodology

4. Methodology for Deriving Stratospheric Column Ozone from SBUV Profiles

A challenge of using SBUV ozone profiles to derive stratospheric column ozone is in determining how to separate the troposphere from the stratosphere given the low resolution of the UV backscatter technique below the ozone peak. The following sections evaluate how dependent the final profile is on the *a priori* profile, how the SBUV final solution profiles compare with ozonesonde measurements, and a description of the empirical correction and its impact on the ozone profiles in the troposphere and lower stratosphere.

4.1 Ozone Profile Data

4.1.1 SBUV Ozone Profiles

The SBUV instrument measures backscattered ultraviolet radiation at 12 different wavelengths to determine total ozone and the vertical ozone profiles. The SBUV instrument was launched on the NASA Nimbus-7 satellite and made measurements from November 1978 through June 1990. A similar record exists from January 1989 through the present from a slightly modified SBUV/2 instrument orbiting on the NOAA-11 satellite. The polar orbiting satellite platform provides global coverage every 6 days. The SBUV data used in the study were derived using the version 6 inversion algorithm and archived as profile layer amounts (see Table 1). Details of the version 6 retrieval algorithm and an error analysis of the SBUV ozone profiles can be found in Bhartia et al. [1996].

4.1.2 Ozonesonde Profile Measurements

The ozonesonde data used in this study were obtained from the ozonesonde database maintained by NASA Langley Research Center [V. Brackett, NASA Langley Research

Center, personal communication, 2004]. Stations chosen for comparison are between are between 50° N and 50° S (see Table 2) and have recurrent ozonesonde measurements between 1979 through 2000: Hohenpeissenberg, Sapporo, Sofia, Boulder, Wallops Island, Tateno, Kagoshima and Naha at northern mid-latitudes; Nairobi and Natal at low-latitudes; and Irene and Lauder at southern mid-latitudes. A detailed description of the station data and the measurement error associated with them are presented in Logan [1999].

4.2 Comparison of Archived SBUV Ozone Profiles with the *a Priori* Profiles in the Troposphere

The UV wavelengths used to determine the ozone profile in the troposphere and lower stratosphere, are also sensitive to aerosols, clouds and ozone over a broad area of the profile. This limits the resolution of the instrument to approximately 15km below the peak, whereas the resolution above the peak is approximately 8 km. The decreased sensitivity to ozone in the lower portion of the profile forces the retrieval algorithm to depend heavily on the *a priori* profile shape and the total ozone amount in determining the final profile below the ozone peak [McPeters et al. 1986]. The version 6 SBUV retrieval *a priori* profiles are classified by total ozone and latitude, and derived from SAGE and ozonesonde profiles. Figure 1 shows a box-and-whisker plot of the NOAA-11 1997 50° S to 50° N first guess ozone profile layers (left panel) and the difference between the final solution profile and first guess profile for each layer (right panel). The graphs show data from over 200,000 profiles. The left and right edges of the box are the upper and lower quartiles of the difference and the line through the middle of the box is the mean. The whiskers extend to the minimum and maximum values. The majority of variability in the profile shape is in layers 2 through 6. It is clear from the left panel in Figure 1 that the *a priori* value of layer one ranges from approximately 20 DU to 25 DU and from the right panel in Figure 1 that the range of the final solution profile is within –2 DU to +6 DU of the first guess value. We will see in the following comparison of SBUV profiles with ozonesonde profiles that the Layer 1 final solution is generally lower than the climatological ozonesonde value and also lacks the seasonal variability seen in the *in*

situ measurements (e.g., see Plates 1 and 2 in Fishman and Balok, 1999). Conversely, the final solution to Layer 3 is nearly always higher than that of the ozonesonde values.

4.3 Comparison of SBUV ozone profiles with Ozonesonde measurements in the troposphere and lower stratosphere

The following results are quantitative comparisons of the combined 16 year Nimbus-7 and NOAA-11 archived SBUV ozone profile data set with greater than 3000 ozonesonde measurements from 12 stations in the troposphere and lower stratosphere. The high-resolution ozone soundings were integrated to obtain the layer amounts listed in Table 1. SBUV profile measurements were required to be within 5 degrees latitude by 5 degrees longitude of the ozonesonde station location and on the same day as the ozonesonde launch. The comparison focuses on Layers 1 through 5. Above 15.8 hPa, the number of ozonesonde measurements decreases significantly due to balloon bursts. Layer 1 represents the amount of ozone in the troposphere. Layer 2 and Layer 3, depending on latitude and season, can be a mix of tropospheric and stratospheric air masses depending on the tropopause height. Layers 4 and 5 are representative of stratospheric concentrations at the ozone profile maximum.

Differences between the SBUV and corresponding ozonesonde layer values for each of the stations are given in Table 3. The mean error in percent units is calculated as the mean of (SBUV-ozonesonde)/ozonesonde, and the mean error in Dobson units is calculated as the mean of (SBUV-ozonesonde). Positive mean error values indicate SBUV is overestimating the amount of ozone in the layer, and negative mean error values indicate SBUV is underestimating the amount of ozone in the layer.

The mean errors above 63.3 hPa in Layers 4 and 5 are all generally within 10% and represent a bias smaller than 10 Dobson Units between SBUV and ozonesonde. The mean errors below 63.6 hPa in layers 1, 2, and 3 are significantly higher. SBUV consistently overestimates the amount of ozone in layer 3 at every station. The mean error ranges from +20 % to +131 % and represents a bias of approximately 5 DU to 16 DU. The mean error of Layer 2 is of similar magnitude to layer 3, but represents a bias of only 0.5 to 6 DU. In Layer 1, the SBUV values underestimate the amount of ozone at all stations except for Nairobi, Kenya and Lauder, New Zealand. The Layer 1 mean error is

also significant ranging from approximately +10 % to –33 % and represents a bias of 1 DU to -15 DU. Of the Northern Hemisphere stations, the mean error in Layer 1 is approximately five times less at Boulder (Colorado) than that at Wallops Island (Virginia). Ozonesondes at Boulder are launched from a higher altitude than at Wallops Island, so the integrated amount of ozone between 1013 hPa and 253 hPa is there less than at Wallops Island. For all stations the mean absolute error is within 1 DU to 3 DU of the mean error. This result gives us some confidence bias is not random. We suggest that the mean errors in layer 1 and layer 3 are due to the summertime photochemical production of ozone that is captured by the *in situ* ozonesonde measurement, but not reflected in the appropriate SBUV ozone layer.

Because of the seasonal nature of tropospheric ozone production, we expect to find a seasonal pattern to the mean error. Figure 2 shows the monthly mean error in Dobson Units for Layer 1 and Layer 3. The mean error is generally a factor of two or more for Northern Hemisphere stations during the summer months, relative to other times of the year. This seasonal mean error is less pronounced at Boulder than the other Northern Hemisphere stations due to its high-altitude location. At the Japanese stations, the mean error in Layer one appears to be shifted towards earlier in the year during the April-May springtime, whereas for the rest of the Northern Hemisphere stations the maximum mean error occurs during the June and July. At Natal (5° S) and Irene (26°S), there is a similar shift in mean error during austral spring (September-November), coincident with the peak of biomass burning. At Nairobi (1° S) and Lauder (45° S), SBUV overestimates the amount of ozone in Layer 1, and there does not appear to be a pronounced seasonality to the mean error. Layer 3 mean errors exhibit the same seasonal pattern, but the sign of the mean error is reversed and, in general, Layer 3 is overestimated. There are statistically significant correlations between the layer-1 and layer-3 mean error at all stations except for Sofia, Boulder, Nairobi, and Natal. At Sofia, Bulgaria, there is a small increase in the amplitude of the error during the summer months of June and July, but there is also an increase in February, which is not reflected in Layer 1. At Nairobi, Kenya and Boulder, Colorado, the seasonality of the mean error is much less pronounced and may be due to these stations being representative of relatively unpolluted regions. Although there is a strong mean error in Layer 1 at Natal, the

amplitude of the mean error in Layer 3 is not comparable. Nairobi is the only station where a small positive correlation is seen between seasonality of the error differences at the two layers, although both layers are in good agreement with the observations.

4.4 Application of Empirical Correction to the SBUV Profiles

We have shown that the amount of ozone in the lower stratosphere from 127 hPa to 63 hPa is consistently overestimated when compared to the ozonesonde climatology, particularly in regions where anthropogenic sources of ozone contribute significantly to the climatology; conversely, the lowest layer in the SBUV profile from 1013 hPa to 253 hPa is consistently lower than the ozone climatology in the same regions. This finding prompted the use of an empirical correction to the SBUV profiles to reduce the seasonal bias in Layer 3 based on a monthly climatology developed by Logan [1999] and described in Fishman et al. [2003]. Since the final solution profile contains no information in the troposphere, we replace the SBUV layer 1 and Layer 2 with the Logan climatology and apply the residual as a correction to the lower stratosphere (layer 3). The tropospheric portion of the profile is prescribed as a function of geographic location and month of the year. It takes into account regional and seasonal tropospheric enhancements that were not included in the version 6 *a priori* ozone profiles based solely on total ozone and latitude. The tropopause height will vary according to global location and time of year and will generally lie within Layer 2 or Layer 3. The empirically corrected ozone profile is then integrated above the NCEP tropopause pressure. The portion of stratospheric ozone in the layer bisected by the tropopause height is determined from a regression model developed using ozonesonde profiles. Having accurate column amounts above Layer 2 and Layer 3 and a climatological representative Layer 1 are imperative for deriving the best possible stratosphere. If Layers 1, 2, or 3 are inaccurate, it is possible that a mean error is passed on to the above column layer. Figure 3 summarizes the mean error between the archived and empirically corrected SBUV layers and corresponding ozonesonde layers for 4 stations ranging in latitude from 47° N to 5° S. The empirical correction has lowered the bias in Layer 3 at all stations.

The empirical correction method assumes that there is useful information in each individual SBUV total column ozone measurement and the ozone profile column amount

above 63 hPa. Although this method would be identical to integrating the Logan climatology to the tropopause pressure and subtracting that integral from the SBUV profile total ozone when the tropopause pressure is greater than 125 hPa, this methodology relies on each individual SBUV total column ozone measurement to compute the SCO to capture the large-scale synoptic patterns that define the stratospheric ozone distribution. Furthermore, it is possible that other perturbations in the profile radiances can cause the overestimation of the lower stratospheric layer, which would not be remedied through the application of the empirical correction. On the other hand, however, we can show that the resultant SCO distribution is an improvement over the SCO derived from archived SBUV profiles. The uniqueness of the SBUV record and the plans for continued SBUV instrument measurements encourages us to continue investigating the value of SBUV ozone profile measurements for determining stratospheric column ozone and its usefulness in the derivation of tropospheric ozone fields in conjunction with total column ozone from TOMS.

5. Validation of SBUV Derived Stratospheric Column Ozone

Although satellite measurements provide much better temporal and spatial resolution than individual ground measurement stations, validation of the resultant distributions is intrinsically challenging. Thus, we have chosen two methods to test the validity of such a data set: Comparison against other independently derived quantities (above) and a comparison with fields derived from another satellite data set which we know correctly captures the vertical structure throughout the stratosphere. For this portion of the validation study, we compare the EC-SBUV SCO with SCO fields derived from SAGE profiles. The results of this comparison are presented below.

5. 1 Comparison of SBUV and SAGE derived stratospheric column ozone fields

Stratospheric ozone profile measurements made from SAGE II from 1985 through the present provide solar occultation measurements of ozone profiles with much higher vertical resolution to derive stratospheric column ozone. The SAGE ozone profile measurements have been shown to be in agreement with ozonesonde measurements within 10% down to the tropopause [Wang et al., 2002]. Figure 4 shows the seasonal

stratospheric ozone climatology derived from integrating high vertical resolution SAGE II profiles above the NCEP tropopause height. Profile measurements from 1985 through 2000 were included except for those in the 3 years following the June 1991 eruption of Mount Pinatubo. The dynamical movement of the tropopause height is the primary determinant of the stratospheric ozone column. The strongest gradients are located in the transition between tropopause heights in the vicinity of strong jet streams. Most of the ozone is located in the stratosphere and the same gradients can also be observed in the total column ozone, particularly in the absence of chemical production in the troposphere. SCO is lower in the tropics due to lower tropopause pressures and therefore less mass in the stratosphere. Outside of the tropics, the tropopause height generally decreases towards the poles. Because the tropopause height is determined from the temperature profile, there are seasonal differences in the stratospheric ozone fields between hemispheres. In the summer hemisphere, stratospheric column ozone values are lower than in the winter hemisphere. Stratospheric column ozone values are larger in the Northern hemisphere in winter (December through February) and spring (March through May), than during the summer (June through August) or fall (September through November) months. The same pattern is seen during the Southern Hemisphere winter and spring (JJA and SON) relative to austral summer and autumn (DJF and MAM). The variability of the position of the mid-latitude jet stream and separation between tropical and mid-latitude air masses results in the stratospheric ozone gradient becoming less zonal outside the tropics. The SCO minimum does not occur exactly at the equator, but rather at the low latitudes of the winter hemisphere.

Figure 5 shows the seasonal stratospheric ozone columns derived from Nimbus-7 SBUV and NOAA-11 SBUV/2 empirically corrected ozone profiles from 1985 through 2000 integrated above the NCEP tropopause height. The SBUV seasonal climatologies show similar patterns of increasing ozone towards the poles, the seasonal shift of the minimum in the tropics, and the zonal asymmetry in the mid-latitudes. Figure 6 shows the differences between the SAGE and the SBUV seasonal climatologies. The greatest absolute differences occur at latitudes greater than 25 degrees in both hemispheres. The most pronounced differences are in the regions over the western Pacific Ocean east of the Asian continent and over the northwestern Atlantic off of the East coast of the United

States and also south of Europe over Northern Africa and western Asia. These features are strongest in DJF and MAM, but generally persist throughout the year. These three large differences coincide with local maxima in the mid-latitude jet stream. The stratospheric ozone gradient captured by SAGE and SBUV are not sufficiently similar so that there are large differences in the fields upon subtraction of one from the other. Figure 7 shows the stratospheric column ozone from SAGE and SBUV averaged over 60 degrees longitude along with the difference. Near 30° N, the gradient in the SBUV ozone is much greater than the slope of the SAGE. The much weaker subtropical jet in the Southern hemisphere leads to better agreement between the SAGE and SBUV fields and explains the hemispheric asymmetry. This finding illustrates the necessity of residual methods used to determine tropospheric ozone being able to derive a stratospheric ozone field with well-defined regimes and accurate representations of the gradients in conjunction with the total column ozone.

Figure 8 highlights improvement of the EC-SBUV SCO over the archived SBUV SCO relative to the SAGE SCO distribution (i.e., the quantity |EC-SBUV – SAGE| - |archived SBUV – SAGE|). Shaded areas indicate where the EC-SBUV climatological value is now closer to the SAGE climatological value. Improvements of more than 5 DU are found over much of the northern hemisphere and over the South Atlantic off the coast of Southern Africa. The region of greatest improvement is over the northern hemisphere during the summer months (JJA). Regions where no improvement is shown are typically in the mid-latitude storm tracks. Above the surface (1000 hPa) at northern mid-latitudes (> 20° N), the Logan climatology is zonally symmetric, and therefore will not reflect higher ozone amounts in the upper troposphere in regions where higher ozone amounts are present due to enhanced outflow from the stratosphere [Beekman et al., 1997].

5.2 Comparisons of SBUV derived stratospheric column ozone with In Situ and Ground-Based Measurements

In this section we compare empirically corrected SBUV SCO with stratospheric columns derived from coincident ground-based total ozone measurements and integrated tropospheric column ozone from ozonesondes using the WMO definition of the thermal tropopause height for each sounding. The total ozone measurements used in this study

(also see Table 2) were obtained from the World Ozone Data Center maintained by Environment Canada. The daily ozone values for all stations except Sofia, Bulgaria were made with Dobson spectrometers. The daily total ozone from Sofia, Bulgaria was measured using a filter ozonometer. A discussion of the different methods and comparisons of the ground-based total ozone measurements with Nimbus-7 TOMS and SBUV measurements can be found in Fioletov et al., [1999].

Figure 8 shows that the largest changes in the empirical correction take place at NH middle latitudes, especially in spring and summer. We compare satellite-derived SCO values with coincident SCO integrals generated at the NH middle latitude ozonesonde sites of Hohenpeissenberg (47°N, 11°E) and Wallops Island (38°N, 75°W). For the data summarized in the Tables 4a and 4b and Figures 9a and 9b, 1347 observations were used for Hohenpeissenberg and 416 for Wallops Island. SAGE profiles that were within 1000 km of the two stations were used in the analysis, resulting in 1031 profiles for Hohenpeissenberg and 1488 profiles for Wallops Island. No coincident time criterion was imposed on the SAGE overpass and ozonesonde launch times, as this would have greatly diminished the number of profiles that could have been used to determine the monthly climatological values. Monthly climatological values were calculated by averaging 17 years of daily SCO fields, interpolated to a 1.0° by 1.25° matrix, at the grid point closest to the ground station location.

Wang et al. [2002] performed a detailed comparison of coincident SAGE and ozonesonde profiles at Hohenpeissenberg. Examination of 329 coincident profiles (i.e., within 24 hours and within ~1000 km) shows that there is generally excellent agreement between 13 and 28 km, where the middle latitude stations are generally within 5% down to 20 km and within 10% down to 10 km. SAGE exhibits a positive bias between 15 and 20 km, which is consistent with our analysis, but the data presented in Table 4a and Figure 9a suggest that this bias is most pronounced in November and December, the only two months where the SAGE-derived and the observed SCO from the Dobson-ozonesonde measurements differ by more than 20 DU. During the rest of the year, the SAGE average is less than 2 DU lower than the measured SCO. Wang et al. did not discuss the seasonality of the differences, probably because of the limited size of their database that required coincident measurements in both space and time.

Without the empirical correction, Table 4a shows that the average monthly difference between the SBUV SCO derived from the Version 6 archive and the measured SCO is 14 DU, nearly twice as large as the difference calculated using SAGE. Every month shows SBUV SCO integrals higher than the observations. On the other hand, with the empirical correction, the agreement between the EC-SBUV SCO and the measured SCO is comparable to the agreement between the SAGE and measured SCO.

Table 4b and Figure 9b summarize the measurements at Wallops Island. The amplitude of the seasonal cycle is less than that at Hohenpeissenberg and is captured by the all three sets of satellite measurements. As with Hohenpeissenberg, the four months of the greatest differences (> 10 DU) between the SAGE and measured SCO, (February, July, September, and November) all show higher SAGE amounts. Without the empirical correction, the SBUV integrals are significantly higher than both the measured and SAGE SCO values. With the correction, the EC-SBUV SCO is once again slightly better than the agreement found between the observed SCO than the SAGE SCO values.

Figure 10 shows monthly mean EC-SBUV SCO values compared with the ground-based/*in situ* SCO at the stations listed in Table 2. For each station, monthly EC-SBUV SCO values (open triangles) are plotted with monthly ozonesonde/ground-based SCO values (stars). Table 5 summarizes the impact of the empirical correction on the data shown in Figure 10 by comparing the corresponding monthly mean error, standard deviation, and root-mean-square error, for the EC-SBUV in these plots with both the ground-based/*in situ* measurements and with the SCO derived from the archived SBUV profiles (not plotted in Figure 10). We see from this table that the empirical correction has reduced the mean error by an overall average of 4 DU. Thus, in addition to improvements at Hohenpeissenberg and Wallops Island described earlier, there is also better agreement of the EC-SBUV SCO with the ground-based/*in situ* SCO than the archived SBUV SCO at almost every station where enough ozonesonde data are available to perform such analyses.

6. Discussion

It is generally agreed that stratospheric ozone distributions derived from SAGE, MLS and HALOE provide better vertical resolution than SBUV and these datasets have

undergone extensive validation [WMO, 1999]. The objective of this study is to show that the resultant SCO fields derived using SBUV data that have been modified by the empirical correction described in Fishman et al. [2003] provide a dataset that is comparable in accuracy to one of these other instruments, SAGE. Validation of the TOR derived from the use of TOMS can only be done by comparing these derived data with measurements from only a handful of available ozonesonde sites. Such studies have already been performed and again, we point to the detailed study by Sun [2002] that summarizes all published techniques prior to the EC-TOR dataset described by Fishman et al. [2003].

Creilson et al. [2003] also showed that the longitudinal gradient at in the EC-TOR distribution at northern middle latitudes was accurately captured by comparing the TCO seasonal cycles at Wallops Island and Hohenpeissenberg derived from ozonesonde data with those derived from EC-TOR data. The differences in the TCO seasonality at these two sites resulted in a difference in the observed monthly gradients between these two locations and this seasonal variation in spatial difference was also observed in the EC-TOR data set. Unfortunately, as seen in this study, these two stations are probably the only two where enough ozonesonde measurements (see Table 2) exist where such an analysis can be performed.

Thus, this study has concentrated on the robust stratospheric ozone dataset to provide additional insight into the accuracy of the resultant EC-TOR fields derived using these SCO fields in conjunction with coincident TOMS total ozone measurements. The SCO fields respond to large scale forcing and it is important that the large-scale features picked up by different instruments are consistent with validation measurements and with each other. If these facts are verifiable, then we can assume that the smaller scale variability, which is solely the result of the greater spatial resolution of TOMS, is, in fact, a true tropospheric feature.

Unlike previous studies that look at TOR information only at low latitudes, this EC-TOR technique provides information at middle latitudes where there are considerably more SAGE and ozonesonde data. We have shown that the SCO derived from SBUV data after the empirical correction has been applied improves the amount of ozone without the correction and also provides excellent agreement with the SCO derived from

the SAGE dataset. The regions of greatest difference between the SCO distributions derived from the two different data sets coincides with regions where the most significant amounts of stratosphere-troposphere exchange is likely taking place, and thus in regions where the height of the tropopause is most difficult to define [Fishman et al., 1990; Pierce et al., 2003].

The TOR dataset discussed in Fishman et al. [2003] is electronically available at http://asd-www.larc.nasa.gov/TOR/data.html and provides monthly maps of TOR for nearly two decades. Both Fishman et al. and Creilson et al. [2003] have discussed facets of the inter-annual variability of the TOR in certain regions of the world; the latter study showing that the inter-annual variability of the amount of tropospheric ozone transported across the Atlantic is correlated with the strength of the North Atlantic Oscillation [Hurrell et al., 2003]. Additional studies examining the inter-annual variability of the amount of tropospheric ozone over India, Africa, and Asia are currently in preparation [Fishman et al., 2004] and suggest that the amount of pollution generated over these tropical and subtropical regions is correlated to various other meteorological teleconnections. The analyses presented in this study showing that the SCO component of the TOR calculation from empirically corrected SBUV measurements is as accurate as SCO distributions derived from SAGE measurements enhances the credibility of the TOR derived from EC-SBUV so that the EC-TOR database can be used with greater confidence for studies of interannual variability.

7. Summary and Conclusions

We have completed an in-depth analysis of the distribution of stratospheric ozone using SBUV profile data that have been modified according to the "empirical correction" described by Fishman et al. [2003]. We have found:

1. The empirical correction improves the calculated SCO relative to the archived SBUV (Version 6) profiles when compared to ozonesonde data;
2. The SCO derived from the EC-SBUV data agree with the ozonesonde data as well as SCO derived from SAGE measurements;
3. The SCO distributions derived from EC-SBUV are similar to those derived from SAGE; and

4. Regions where the SAGE and SBUV distributions differ the most are in locations where strong jet stream activity is taking place, suggesting that neither dataset can provide as accurate a data set as desired.

The study by Sun [2002] has already provided a comprehensive analysis of the utility and the limitations for a number of studies that use a residual technique to infer tropospheric ozone from TOMS total ozone measurements. The EC-TOR dataset described in Fishman et al. [2003] was not included in that analysis, but, in general, the same large-scale patterns seen in Fishman et al. [1990] and subsequent residual methods again show up in TOR depictions in the 2003 paper. The primary difference is the much higher spatial resolution highlighted in EC-TOR data, which is due to the much greater number TOMS measurements used in the EC-TOR method.

Subsequently, deLaat and Aben [2003] questioned some of the aspects of Fishman et al. [2003] stating incorrectly that the use of the Logan [1999] ozone climatology should yield the same Logan climatology when the EC-TOR fields are generated. If only SBUV measurements were used to generate a tropospheric residual distribution, then deLaat and Aben would be correct in their assertion. The Logan climatology, however, is used **only** to modify the distribution of ozone in the stratosphere; all tropospheric ozone information is derived solely from TOMS measurements. Thus, the critical question is: How has applying the empirical correction changed the distribution of ozone in the stratosphere? This paper has shown conclusively that the resultant stratospheric distribution has been changed in such a way that the new distribution agrees better with both *in situ* measurements and with the distribution of the SCO derived from SAGE measurements.

8. Acknowledgements

SBUV/2 data were obtained from NOAA/NESDIS with support from the NOAA Climate and Global Change Program Atmospheric Chemistry Element.

9.References

Beekman ,M., et al., Regional and Global Tropopause Fold Occurrence and Related Ozone Flux Across the Tropopause, *J. Atmos. Chem.*, **28**, 29-44, 1997

Bhartia, P.K., R.D. McPeters, C.L. Mateer, L.E. Flynn, C. Wellemeyer, Algorithm for the estimation of vertical ozone profiles from the backscatter ultraviolet technique, J. Geophys. Res., 101(D13), 18,793-18,806, 1996.

Chatfield, R.B., and H. Harrison, Tropospheric ozone 2: Variations along a meridional band, J. Geophys. Res., 82, 5969-5976, 1977.

Creilson, J., J. Fishman, A.E. Wozniak, Intercontinental transport of tropospheric ozone: a study of its seasonal variability across the North Atlantic utilizing tropospheric ozone residuals and its relationship to the North Atlantic Oscillation, Atmospheric Chemistry and Physics, Vol. 3, pp 2053-2066, 25-11-2003.

Crutzen, P.J., Photochemical reactions initiated by and influencing ozone in unpolluted tropospheric air, Tellus, 26(1-2), 47-57, 1974.

DeLaat, A.T.J., and I. Aben, Problems regarding the tropospheric O3 residual method and its interpretation in Fishman et al. (2003), Atmos. Chem. Phys. Discuss. **3**, 5777-5802, 2003.

Fabian, P., and P.G. Pruchniewicz, Meridional distribution of tropospheric ozone from ground-based registrations between Norway and South Africa, Pure Appl. Geophys., 106(5-7), 1027-1035, 1973.

Fabian, P., and P.G. Pruchniewicz, Meridional distribution of ozone in the troposphere and its seasonal variations, J. Geophys. Res., 82(15), 2063-2073, 1977.

Fioletov, V.E, J.B. Kerr, E.W. Hare, G.J. Labow, R.D. McPeters, An assessment of the world ground-based total ozone network performance from the comparison with satellite data, J. Geophys. Res., 104(D1), 1737-1747, 1999.

Fishman, J., and A.E. Balok, Calculation of daily tropospheric ozone residuals using TOMS and empirically improved SBUV measurements: Application to an ozone pollution episode over the eastern United States, J. Geophys. Res., 104, 30,319-30,340, 1999.

Fishman, J., and Crutzen, P.J. The origin of ozone in the troposphere, Nature, 274, 855-858, 1978.

Fishman, J., S. Solomon and P.J. Crutzen, Observational and theoretical evidence in support of a significant in-situ photochemical source of tropospheric ozone, Tellus, 31, 432-446, 1979.

Fishman, J., C.E. Watson, J.C. Larsen, and J.A. Logan, Distribution of tropospheric ozone determined from satellite data, J. Geophys. Res., 95, 3599-3617, 1990.

Fishman, J., V.G. Brackett, E.V. Browell, and W.B. Grant, Tropospheric ozone derived from TOMS/SBUV measurements during TRACE-A, J. Geophys. Res., 101, 24,069-24,082, 1996a.

Fishman, J., J.M. Hoell, Jr., R.D. Bendura, R.J. McNeal, and V.W.J.H. Kirchoff, NASA GTE TRACE-A experiment (September-October 1992): Overview, J. Geophys. Res., 101, 23,865-23,879, 1996b.

Fishman, J., A.E. Wozniak, J.K. Creilson, Global distribution of tropospheric ozone from satellite measurements using the empirically corrected tropospheric ozone residual technique: Identification of the regional aspects of air pollution, Atmos. Chem. Phys., 3, 893-907, 2003.

Fishman, J., J.K. Creilson, and A.E. Wozniak, An Investigation of tropospheric ozone interannual variability over Africa determined from satellite measurements, Presented at Spring 2004 AGU Meeting, Montreal, Quebec, Canada, May 17-21, 2004.

Hudson, R.D., and A.M. Thompson, Tropical tropospheric ozone from Total Ozone Mapping Spectrometer by a modified residual method, *J. Geophys Res*., 103, 22,129-22,145, 1998.

Hurrell, J.W., Y. Kushnir, G. Ottersen, and M. Visbeck, Eds., *The North Atlantic Oscillation: Climate Significance and Environmental Impact, 2003.* Geophysical Monograph Series, **134**, American Geophysical Union, Washington, 279pp., 2003.

Kaye, J.A., and J. Fishman, Stratospheric ozone observations; in Handbook of Climate, Weather, and Water: Chemistry, Impacts, and Applications, T.D. Potter and B. Colman, Eds.; Wiley, New York, 385-404,2003.

Logan J.A., An analysis of ozonesonde data for the troposphere: Recommendations for testing 3-D models, and development of a gridded climatology for tropospheric ozone, J. Geophys. Res., 104(D13), 16,115-16,149, 1999.

McPeters, R.D., D.F. Heath, P.K. Bhartia, Average ozone profiles for 1979 from the NIMBUS 7 SBUV instrument, Geophys. Res. Lett., 13, 1213-1216,1986.

McPeters, R.D., T. Miles, L.E. Flynn, C.G. Wellemeyer, J.M. Zawodny, Comparison of SBUV and SAGE II ozone profiles: Implications for ozone trends, J. Geophys. Res., 99(D10), 20,513-20,524, 1994.

Newchurch, M. J., X. Liu, J. H. Kim, Lower-tropospheric ozone (LTO) derived from TOMS near mountainous regions, *J. Geophys. Res., 106,* 20, 403-412, 2001.

Newchurch, M.J., D. Sun, J.H. Kim, and X. Liu, Tropical Tropospheric Ozone Derived using Clear-Cloudy Pairs (CCP) of TOMS Measurements, *Atmospheric Chemistry and Physics*, *3*, 683-695, 2003.

Prinn, R.G., Toward an improved network for determination of tropospheric ozone climatology and trend, J. Atmos. Chem., 6(3), 281-298, 1988.

Sun, D., Tropical tropospheric ozone: New methods, comparisons, and model evaluation of controlling processes, Dissertation, Dept. Atmos. Sci., Univ. Alabama, Huntsville, 174 pp., 2002.

Vukovich, F.M., V. Brackett, J. Fishman, and J.E. Sickles, II, On the feasibility of using the tropospheric ozone residual for nonclimatological studies on a quasi-global scale, J. Geophys. Res., 101(C4), 9093-9105, 1996.

Vukovich, F.M., V. Brackett, J. Fishman, and J.E. Sickles, II, A 5-year evaluation of the tropospheric ozone residual at nonclimatological periods, J. Geophys. Res, 102(D13), 15,927-15,932, 1997.

Wang, H. J., D. M. Cunnold, L. W. Thomason, J. M. Zawodny, and G. E. Bodeker, Assessment of SAGE version 6.1 ozone data quality, J. Geophys. Res., 107(D23), 4691, doi:10.1029/2002JD002418, 2002.

WMO, 1999: Scientific Assessment of Ozone Depletion: 1998. Global Ozone Research and Monitoring Project - Report No. 44, World Meteorological Organization, Geneva, Switzerland, 732 pp.

WMO, 2003: Scientific Assessment of Ozone Depletion: 2002. Global Ozone Research and Monitoring Project - Report No. 47, World Meteorological Organization, Geneva, Switzerland, 498 pp.

Ziemke, J.R., and S. Chandra, and P.K. Bhartia, Two new methods for deriving tropospheric column ozone from TOMS measurements: Assimilated UARS MLS/Haloe and convective-cloud differential techniques. *J. Geophys. Res*., 103, 22,115-22,127, 1998.

Table 1. Definition of SBUV Ozone Profile Layers

SBUV Layer	Pressure Range (hPa)	Midpoint Pressure (hPa)	Approx. Midpoint Altitude (km)
1	253-1013	507	5.5
2	127-253	179	12.5
3	63.3-127	89.6	17.0
4	31.7-63.3	44.8	21.3
5	15.8-31.7	22.4	25.8
6	7.92-15.8	11.2	30.4
7	3.96-7.92	5.60	35.2
8	1.98-3.96	2.80	40.2
9	0.99-1.98	1.40	45.4
10	0.495-.099	0.700	51.0
11	0.247-0.495	0.350	56.5
12	0.0-0.2467	-	-

Table 2. Individual Stations with Ozonesonde and Ground-Based Total Ozone Measurements

WMO ID	Station Name	Latitude	Longitude
099	Hohenpeissenberg, Germany	47.80 N	11.02 E
012	Sapporo, Japan	43.05 N	141.33 E
132	Sofia, Bulgaria	42.81 N	23.38 E
067	Boulder, Colorado, USA	40.03 N	105.25 W
014	Tateno, Japan	36.05 N	140.13 E
107	Wallops Island, Virginia, USA	37.93 N	75.48 W
007	Kagoshima, Japan	31.55 N	130.55 E
190	Naha, Japan	26.20 N	127.68 E
175	Nairobi, Kenya	1.27 S	36.80 E
219	Natal, Brazil	5.42 S	35.38 W
265	Irene, Pretoria, South Africa	25.90 S	28.22 E
256	Lauder, New Zealand	45.03 S	169.68 E

Table 3. Mean Error (ME) between Archived SBUV (Version 6) and Ozonesondes from 1013 hPa to 15.8 hPa

		Layer 1		Layer 2		Layer 3		Layer 4		Layer 5	
Station	Matches	%	DU	%	DU	%	DU	%	DU	%	DU
Hohenpeissenberg, GR	1617	-14.68	-5.42	11.04	-0.03	28.58	11.99	-7.68	-6.37	3.66	2.12
Sapporo, Japan	238	-17.78	-6.74	36.03	5.72	45.35	15.93	-2.75	-2.61	2.98	1.73
Sofia, Bulgaria	133	-33.37	-14.34	-3.01	-2.16	24.73	9.50	-10.39	-8.98	0.72	-0.90
Boulder, CO, USA	453	-6.58	-2.65	47.96	2.00	57.66	12.55	12.36	-6.71	2.44	0.68
Wallops Island, VA, USA	413	-33.56	-13.12	39.38	2.19	37.42	10.10	-11.12	-8.67	0.27	-0.21
Tateno, Japan	356	-29.52	-10.91	48.10	4.38	66.89	15.81	-2.98	-3.21	2.39	1.30
Kagoshima, Japan	226	-24.61	-8.88	68.51	4.98	97.35	14.46	-1.13	-1.61	3.32	1.86
Naha, Japan	224	-12.52	-5.47	75.40	3.96	131.54	12.75	5.19	1.61	5.53	3.53
Nairobi, Kenya	102	10.62	1.14	31.19	1.16	53.47	4.63	-0.48	-0.54	2.99	1.94
Natal, Brazil	303	-13.08	-5.22	20.94	0.46	56.27	4.83	6.97	2.32	5.80	3.31
Irene, South Africa	65	-18.14	-5.84	19.43	1.83	49.43	7.87	-11.04	-7.46	-10.59	-8.51
Lauder, New Zealand	248	4.30	0.41	4.49	-1.58	20.24	7.29	4.82	3.15	-9.53	-6.60

Table 4a. Seasonal Cycle of Observed SCO over Hohenpeissenberg Compared with SCO Derived from Satellite Measurements

Month	SCO[1]	SAGE	|Diff|	SBUV	|Diff|	EC-SBUV	|Diff|
Jan	302	307	5	306	4	301	1
Feb	321	311	10	329	8	323	2
Mar	338	342	4	339	1	331	7
Apr	338	338	0	350	12	340	2
May	324	322	2	343	19	330	6
Jun	307	294	13	327	20	314	7
Jul	291	285	6	307	16	294	3
Aug	278	276	2	292	14	282	4
Sep	258	264	6	277	19	266	8
Oct	254	256	2	267	13	258	4
Nov	251	272	21	268	17	259	8
Dec	268	290	22	288	20	282	14
Average	294	296	8	308	14	298	6

[1]Dobson-Ozonesonde
All values given in Dobson Units.

Table 4b. Seasonal Cycle of Observed SCO over Wallops Island Compared with SCO Derived from Satellite Measurements

Month	SCO[1]	SAGE	|Diff|	SBUV	|Diff|	EC-SBUV	|Diff|
Jan	285	280	5	290	5	285	0
Feb	286	304	18	301	15	293	7
Mar	304	303	1	314	10	306	1
Apr	308	310	2	320	12	308	0
May	293	299	6	313	20	300	7
Jun	285	281	4	294	9	282	3
Jul	264	274	10	279	15	271	7
Aug	258	259	1	272	14	267	9
Sep	246	257	11	263	17	257	11
Oct	250	257	7	259	9	253	3
Nov	244	258	14	256	12	249	5
Dec	268	262	6	272	4	266	2
Average	274	279	7	286	12	278	5

[1]Dobson-Ozonesonde
All values given in Dobson Units.

Table 5. Monthly Mean Error, Standard Deviation, and RMSE for Stratospheric Column Ozone

	Empirically Corrected-SBUV			SBUV from V6 Archive		
Station	ME (DU)	SDE (DU)	RMSE (DU)	ME (DU)	SDE (DU)	RMSE (DU)
Hohenpeissenberg, GR	2.27	4.24	4.66	11.60	5.73	12.83
Sapporo, Japan	4.73	7.47	8.57	10.64	9.56	14.03
Sofia, Bulgaria	-10.35	6.31	11.98	-2.21	8.64	8.56
Boulder, CO, USA	-0.33	6.63	6.35	9.60	5.95	11.16
Wallops Island, VA, USA	3.33	3.82	4.94	11.20	2.59	11.47
Tateno, Japan	10.91	6.22	12.61	18.38	7.74	19.82
Kagoshima, Japan	6.17	7.45	8.58	12.75	6.68	14.27
Naha, Japan	8.61	8.61	11.18	13.03	8.29	15.26
Nairobi, Kenya	-1.12	3.46	3.50	1.24	1.71	2.05
Natal, Brazil	2.52	3.55	4.23	6.21	4.45	7.54
Irene, South Africa	5.60	2.10	5.95	7.78	2.49	8.14
Lauder, New Zealand	7.96	6.15	9.90	7.83	5.00	9.18

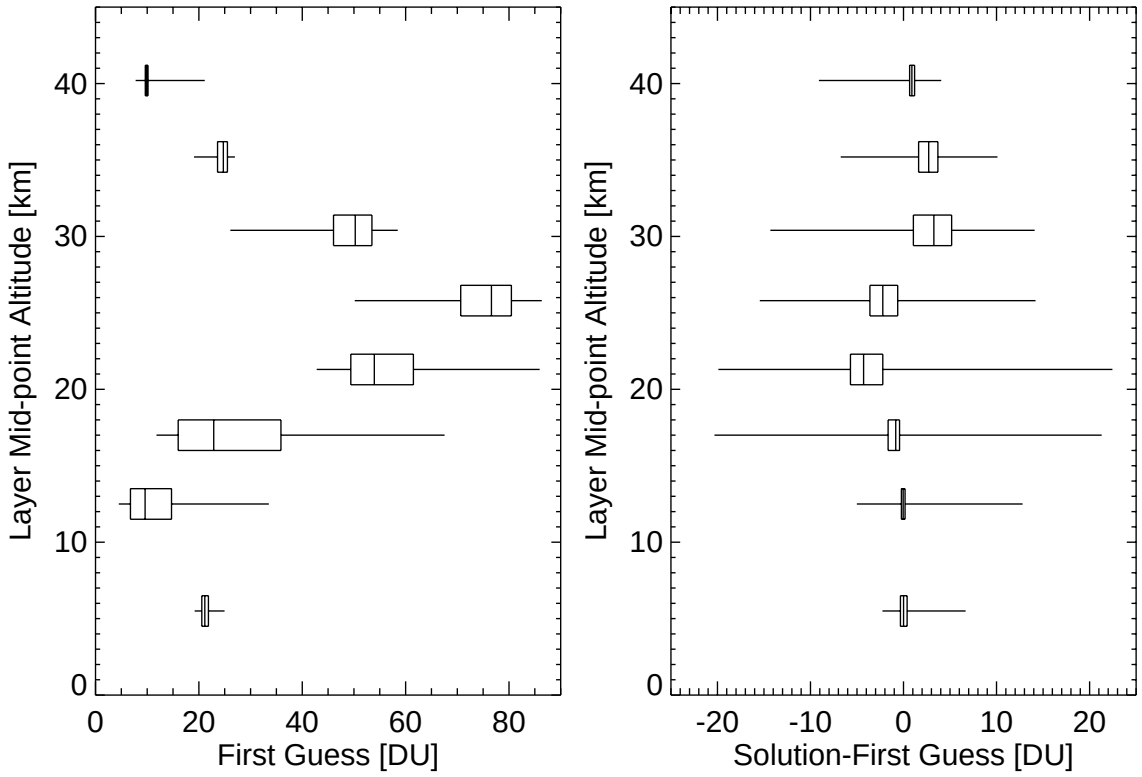

Figure 1. A box-and-whiskers plot of the NOAA-11 1997 50° S to 50° N first guess profile layers as a function of layer mid-point altitude (left panel). The left and right edges of the box show the lower and upper quartiles, respectively. The line through the middle of the box shows the median value and the whiskers show the minimum and maximum values for each layer. The right panel shows a box-and-whiskers plot for the difference between the final solution profile and first guess profile (final solution-first guess) for each layer.

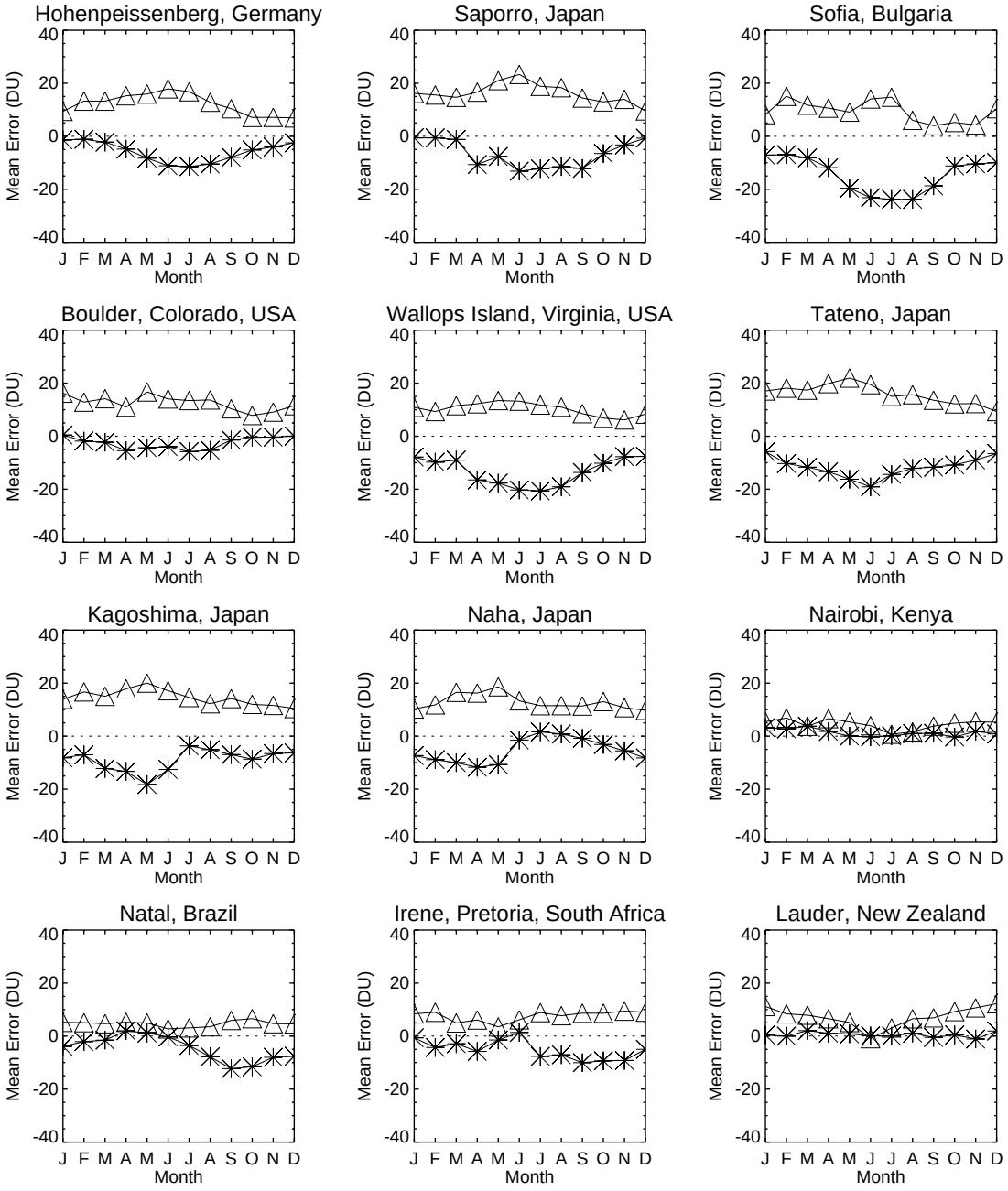

Figure 2. Monthly mean error of SBUV profiles compared with ozonesonde profiles (SBUV-ozonesonde) in Layer 1 and Layer 3. Triangles are the mean error for Layer 3 and the stars are the mean error for Layer 1.

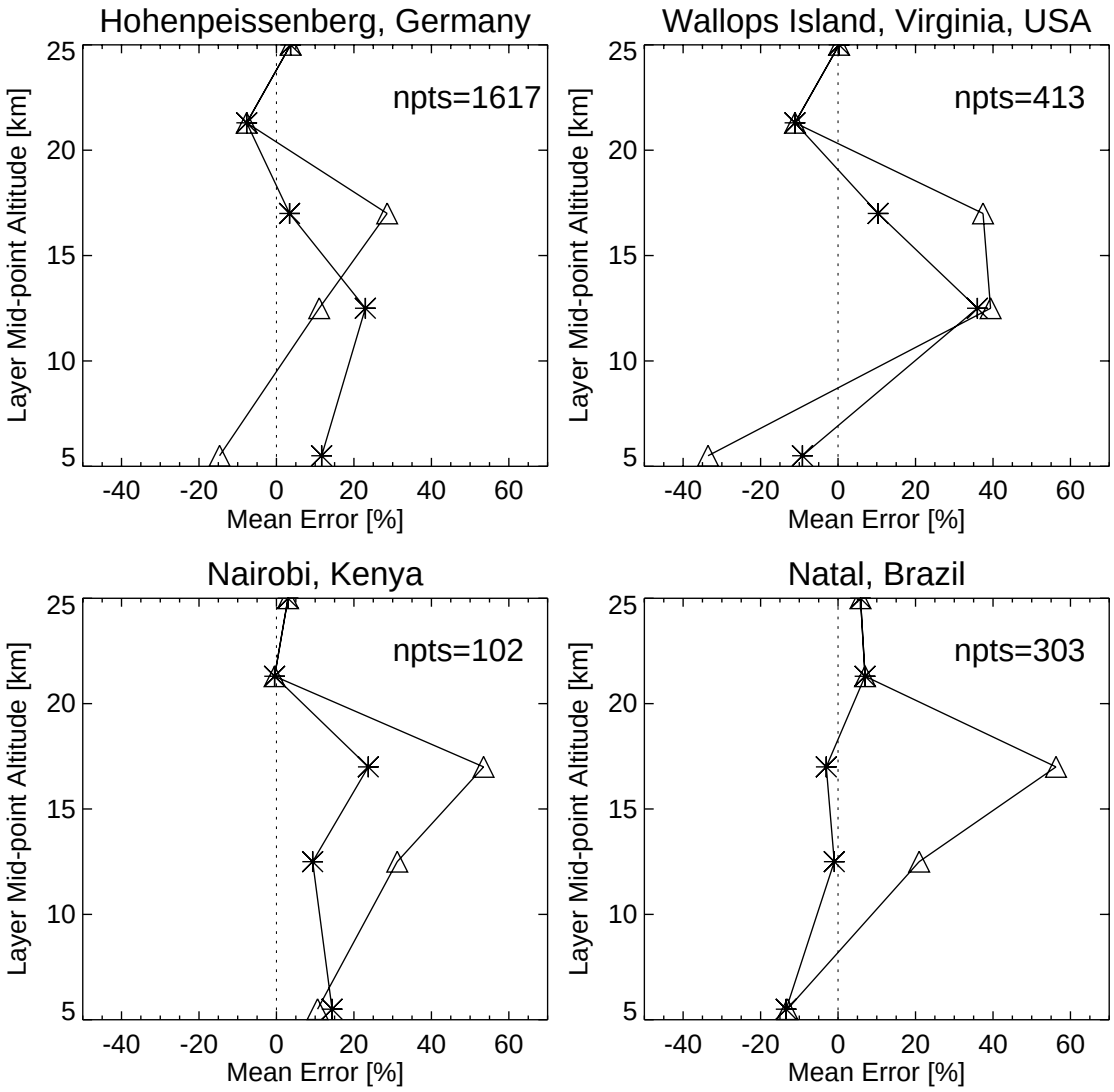

Figure 3. Mean bias of SBUV profiles compared with ozonesonde profiles ((SBUV-ozonesonde)/ozonesonde) for Layers 1-5 at 4 locations. Triangles are uncorrected SBUV profiles and stars and corrected SBUV profiles.

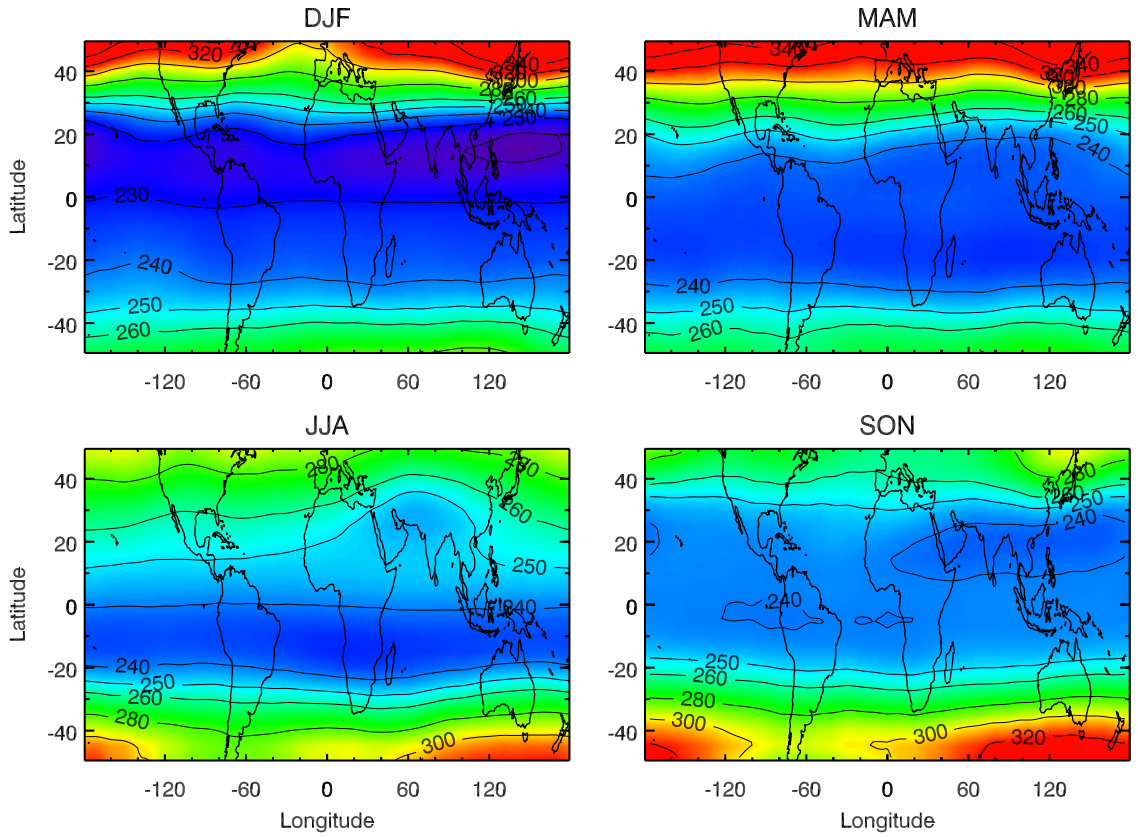

Figure 4. Seasonal stratospheric column ozone distribution derived from SAGE II (1985-2000) ozone profiles.

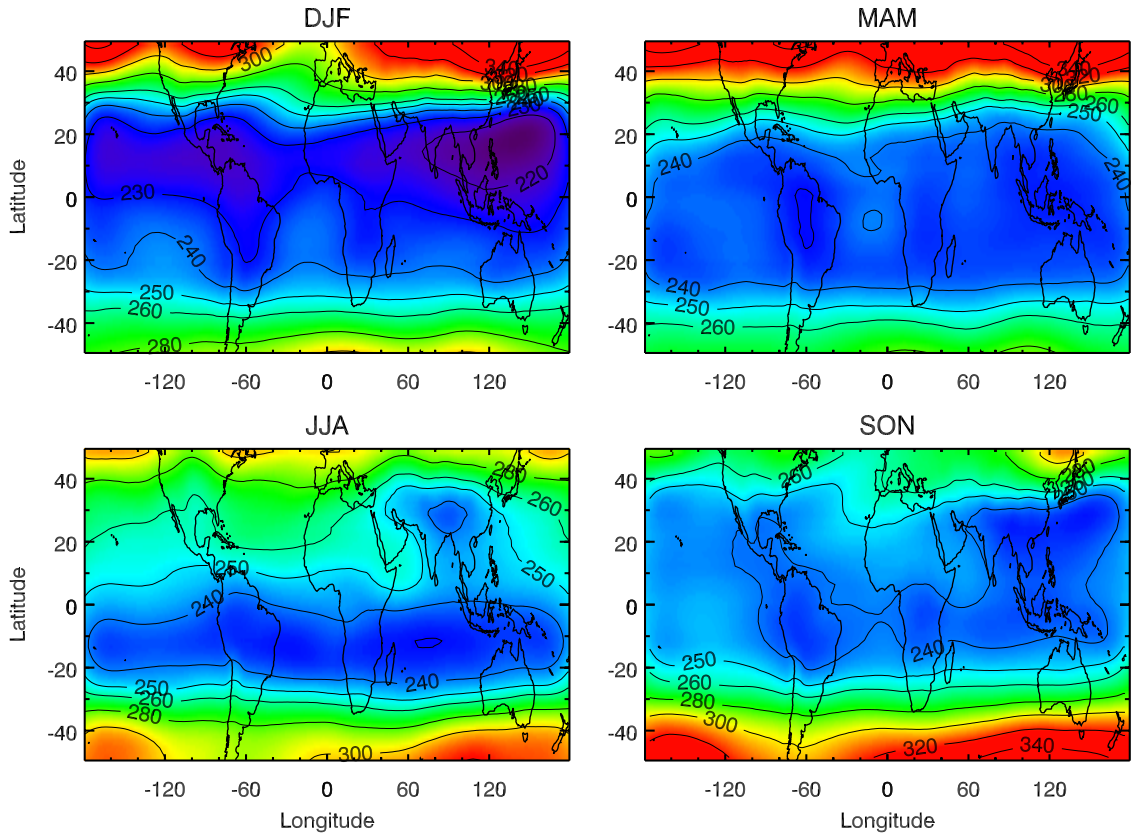

Figure 5. Same as Figure 4 except using data from empirically corrected SBUV measurements from 1979 through 2000.

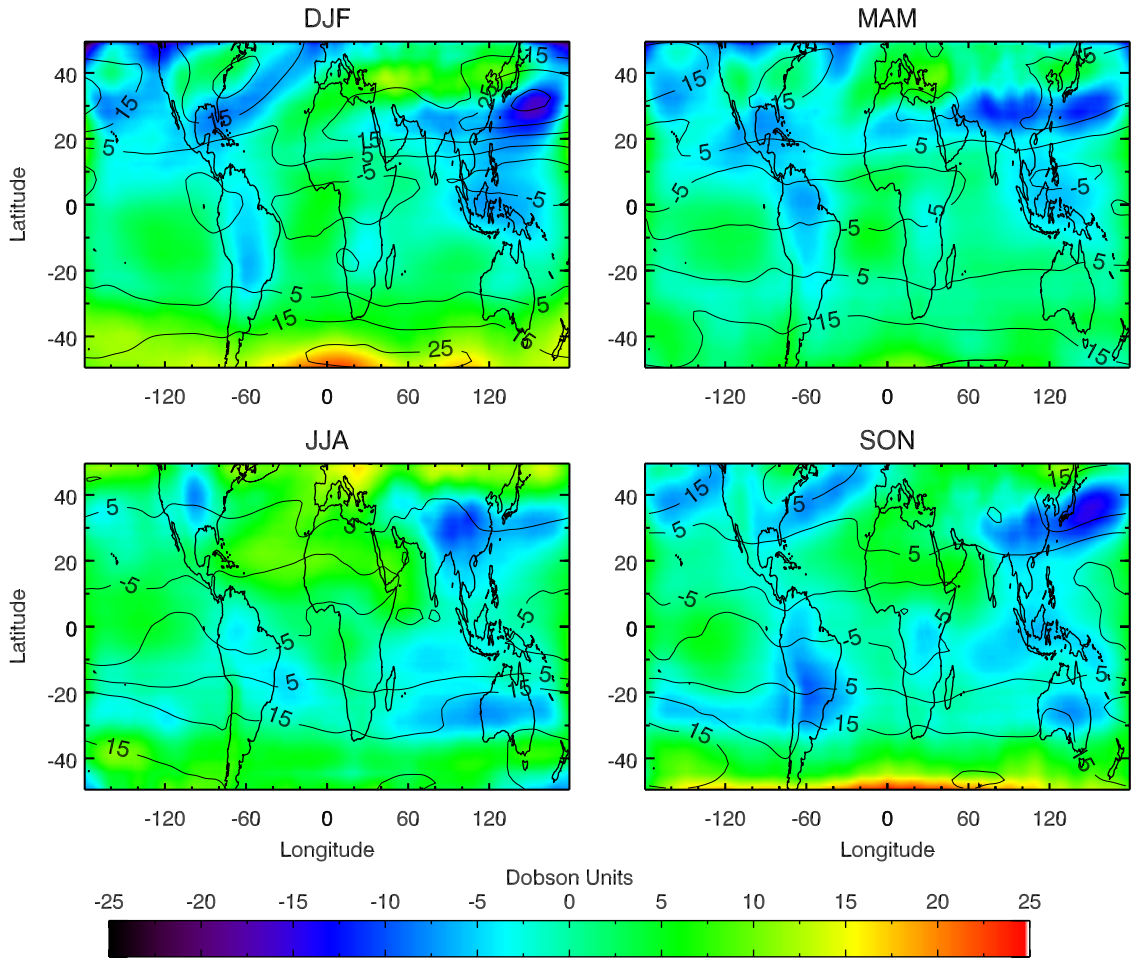

Figure 6. Difference between SBUV and SAGE (SBUV-SAGE) stratospheric column ozone fields with contours of 500-hPa u-wind in m/s overlaid onto the ozone field.

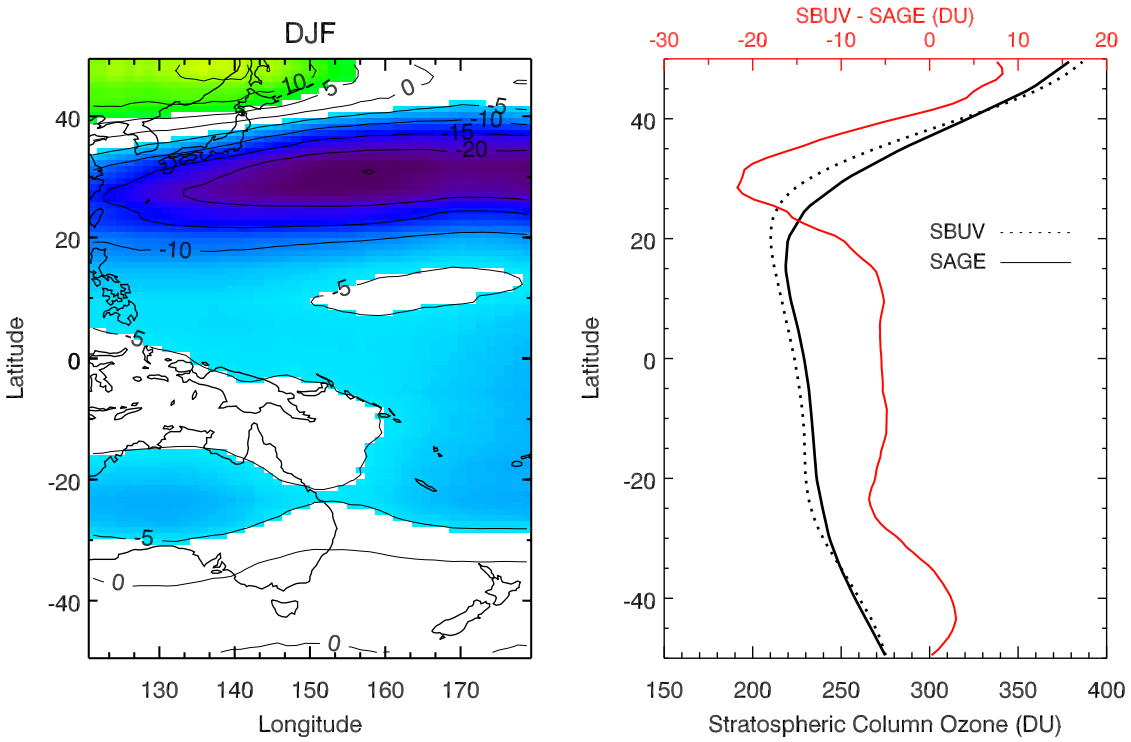

Figure 7. The left panel shows the difference between the DJF SBUV and SAGE (SBUV-SAGE) stratospheric column ozone fields. The right panel shows the mean cross-section of SBUV (dotted black line) and SAGE (solid black line) stratospheric column ozone, and the difference (SBUV-SAGE) (solid red line).

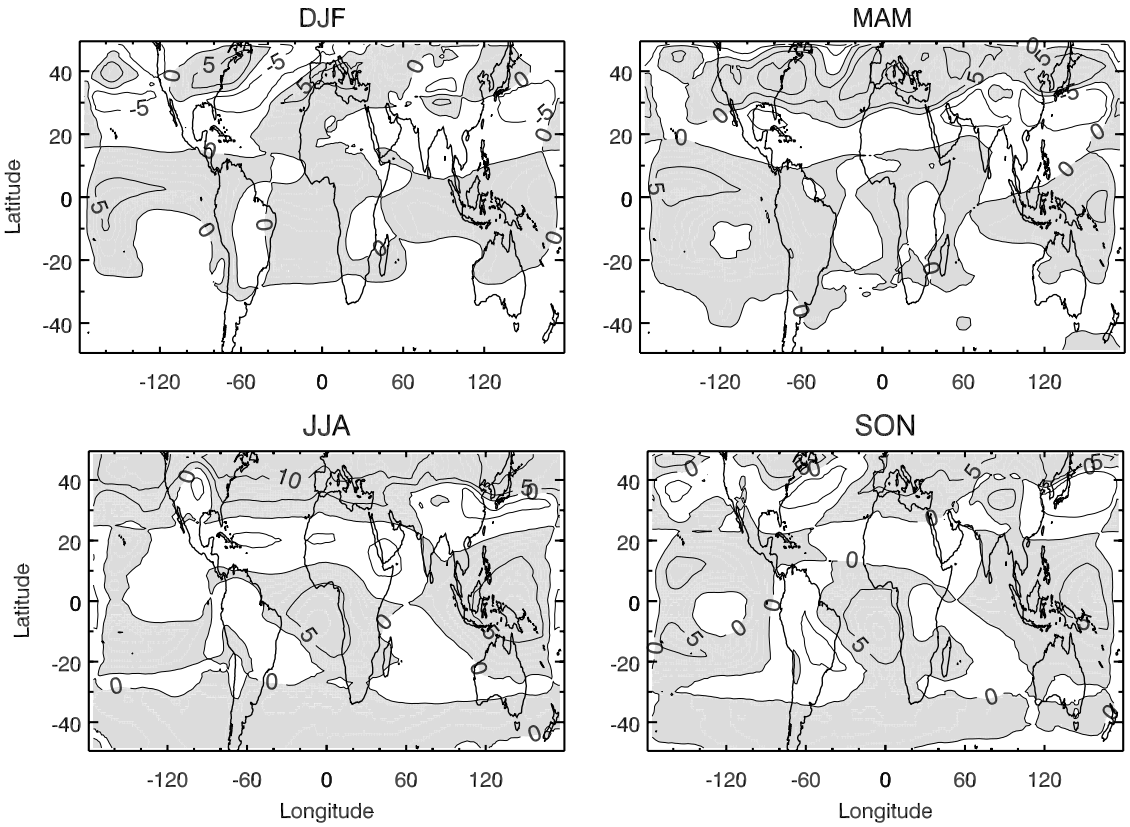

Figure 8. Distribution of |(EC-SBUV-SAGE)| – |(SBUV-SAGE)| Shaded regions show where the empirical correction has brought the SBUV fields closer to the stratospheric column ozone fields generated using SAGE measurements.

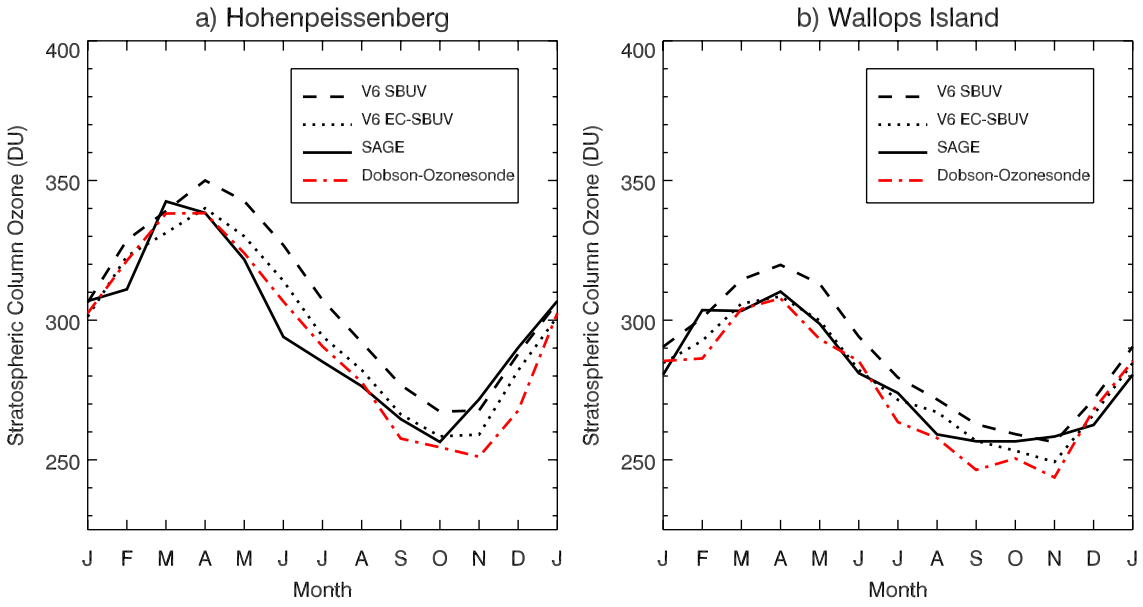

Figure 9. Seasonal cycle of SCO at Hohenpeissenberg, GR and Wallops Island, USA. The Dobson-ozonesonde values are plotted as thick dash-dot (red) line; the satellite-derived (black) lines show SAGE SCO (thin solid) and SBUV SCO (dashed) and the EC-SBUV SCO (dotted).

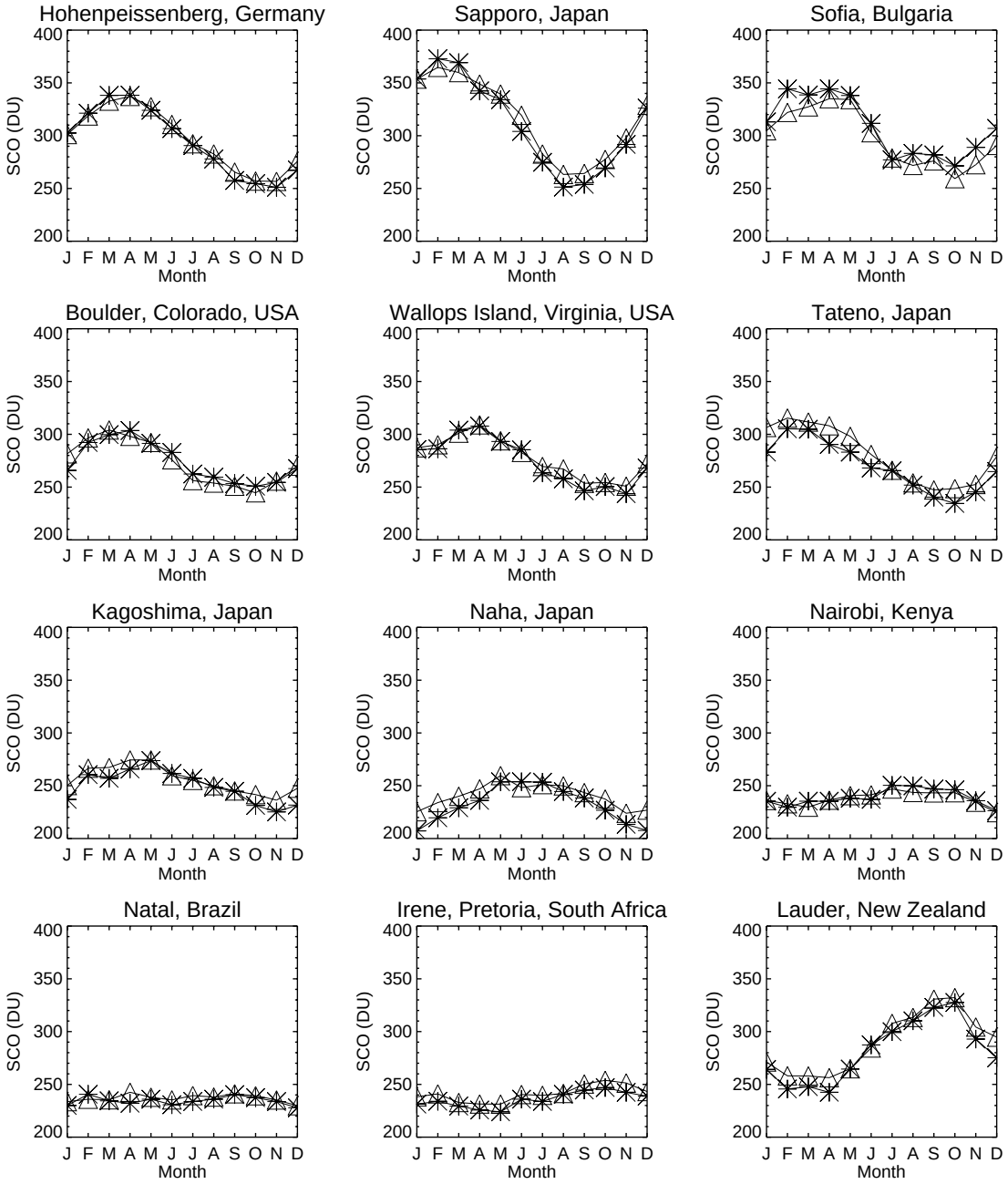

Figure 10. Monthly mean stratospheric column ozone derived from EC-SBUV and Dobson-ozonesonde measurements. The triangles are the EC-SBUV SCO and the stars are Dobson-ozonesonde SCO.